International Conference on Hydrodynamic Instability and Turbulence

Proceedings of ICHIT- 06
26 February – 5 March 2006, Moscow, Russia

DIRECT NUMERICAL SIMULATION OF TURBULENT RAYLEIGH-BENARD CONVECTION

Igor B. Palymskiy

Modern Academy for Humanities, Novosibirsk Branch , Novosibirsk, Russia, 630064

palymsky@hnet.ru

ABSTRACT

Turbulent convectional flow of water in horizontal layer with free and rigid horizontal boundaries, arising by heating from below, is numerically simulated by spectral method using the Boussinesq model without any semiempirical relationships (DNS) in 2-D case. The results of the both numerical simulations compare with experimental data. We studied the time and space spectrums of temperature pulsations and kinetic energy in both free and rigid simulations. The Kolmogorov ($k^{-5/3}$), Obukhov-Bolgiano ($k^{-7/5}$ for temperature pulsations and $k^{-11/5}$ for kinetic energy of pulsations) spectrums have been derived in numerical simulations. These spectrums were observed earlier in experimental investigations of turbulent convection of gaseous He. It is surprising that ranges of $k^{-5/3}$ and $k^{-7/5}$ spectrums are partially coincident.

INTRODUCTION

At last time many workers have studied thermal Rayleigh-Benard convection using numerical simulation. As rule, they used spectral methods with periodic boundary conditions. In numerical simulations were derived stationary, periodic, quasiperiodic and stochastic regimes [1]. Some authors performed 2-D and 3-D simulations for high supercriticality with free [2,3] and rigid [4,5] boundary conditions on the horizontal planes. The results of correct performed 3-D numerical simulations with rigid boundary conditions in air, as rule, have good agreement with experimental data ([6] and [7], for instance). But we have a big troubles with deriving of time-dependent solutions for 2-D convection in air and gaseous He, up to large Rayleigh number all solutions are steady state [4].

On the other hand, it is revealed recently that the time-dependent solutions of 2-D convection with free boundary conditions (stress free) at Prandtl number is equal to 10 have a good agreement with experimental data on turbulent convection in air and gaseous He [8]. It is very significant and practical, as using of free boundary conditions very simplifies the DNS of turbulent convection, simple and efficient numerical algorithms have been generated using the formulas of linear stability theory [9,10].

For instance, in table 1 we compare the calculating Nusselt numbers. Here and below $r = Ra/Ra_{cr}$ is supercriticality, when Ra and Ra_{cr} are Rayleigh number and the critical value of Rayleigh number, respectively.

Table 1
Comparing of Nusselt Number at r = 33000

[4], 2-D, rigid, water	24.8
[11], experiment, gaseous He	25.2
[12], experiment, air	27.5
[2], 3-D, free, air	33.0
Present, 2-D, free, water	28.7

The same situation you can see in [8] for r = 9800.It shows that for simulations with free boundary conditions the value of Prandtl number must be higher because of decreasing of effective Prandtl number by free boundary conditions.

The aim of this work is more detailed comparing of results of 2-D simulations with free and rigid boundary conditions on horizontal planes with experimental data on turbulent convection.

PROBLEM FORMULATION

Turbulent convectional flow of water in a horizontal layer numerically is simulated by heating from below. The fluid is viscous and incompressible. The flow is time-dependent and two-dimensional. Boundaries of a layer are isothermal and free (stress-free) or rigid. The model Boussinesq is used without semiempirical relationships. The dimensionless system of equations in terms of deviations from an equilibrium solution, representation of problem solution in the form of sum of eigenfunctions of linear stability theory, the boundary conditions, the special numerical method, testing and the results of linear and non linear analysis (on model non linear system) for free boundary conditions are described in works [9, 10]. In our simulations with free boundary conditions we used up to 257*63 harmonics at supercriticality up to r = 34000. In the test simulations we used up to 513*127 of harmonics with free boundary conditions.

For simulations with rigid boundary conditions we used the spectral representation in x-direction and finite differences in y-direction with uniform mesh. We used up to 257 harmonics in x-direction and 65 points in y-direction at supercriticality up to 7000. In the test simulations we used up to 513*65 (or 257*129) of harmonics with rigid boundary conditions.

We simulated the convection flows for the Prandtl number Pr is equal to 10, for all simulations the dimensionless periodicity interval is equal to 2π, the dimensionless distance between the planes is equal to 1.

So, we are solving the system of equations

$$\begin{aligned} &\omega_t + \frac{1}{\Pr}(\varphi_y \omega_x - \varphi_x \omega_y) = \Delta\omega + Ra\mathrm{Q}_x, \\ &\Delta\varphi = -\omega, \qquad\qquad (1) \\ &\mathrm{Q}_t + \frac{1}{\Pr}(\varphi_y \mathrm{Q}_x - \varphi_x \mathrm{Q}_y) = \frac{1}{\Pr}\Delta\mathrm{Q} - \frac{1}{\Pr}\varphi_x, \end{aligned}$$

where φ is a stream function, ω is the vortex, Q is the temperature deviation from equilibrium profile (the total temperature being T = 1 - y + Q), $\Delta f = f_{xx} + f_{yy}$ is the Laplace operator, $Ra = g\beta H^3 dQ/\chi\nu$ is the Rayleigh number, Pr = ν/χ is the Prandtl number, g is the gravitational acceleration, β, ν, χ are the coefficients of thermal expansion, kinematics viscosity and thermal conductivity, respectively, H is the layer height and dQ is the temperature difference on the horizontal boundaries.

RESULTS AND DISCUSSION

Fig.1 represents the average temperature profile. At figs. 1 - 4 below y denotes transverse coordinate. At fig.1 symbol ● denotes experimental results [7] (r = 5900, air), dash line – experimental results [13] (r = 5500, water), solid line - results of present work with free boundary conditions (r = 6000, Pr = 10).

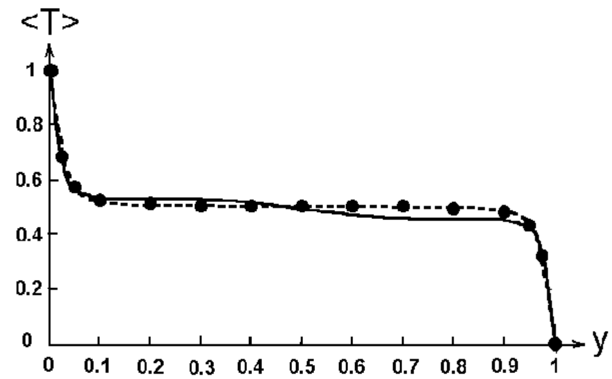

Figure 1
Average temperature profile at r = 6000

Fig.2 represents the rms of vertical velocity pulsations. Here symbol ● denotes the experimental results [7] (r = 5900, air), symbol ■ – experimental result [12] (r = 5900, air), solid line - results of present work with free boundary conditions (r = 5500, Pr = 10).

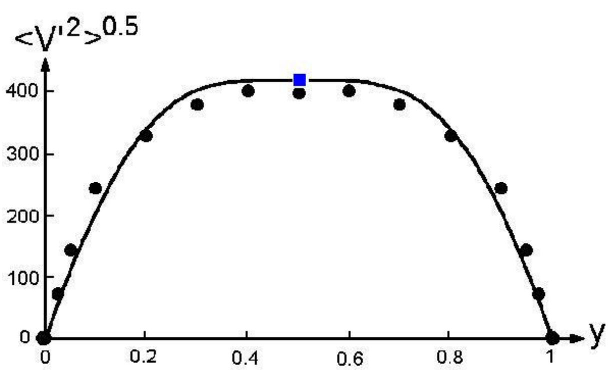

Figure 2
Rms of vertical velocity pulsations at r = 6000

Fig.3 represents the rms of temperature pulsations at moderate supercriticality r = 1250. Here symbol ● denotes the experimental results [7] (r = 1470, air), symbol □ – experimental result [12] (r = 1400, air), symbol ◊ - experimental result of Somerscales, 1965 (r = 1170, data is from work [7]), symbol ○ – experimental result [14] (r = 1250, gaseous He), solid line - results of present work with free boundary conditions (r = 1250, Pr = 10). The experimental data has a big scatter and derived numerical results have a reasonably good agreement with experimental data, some waviness is coupled possibly with Gibbs effect for spectral representations.

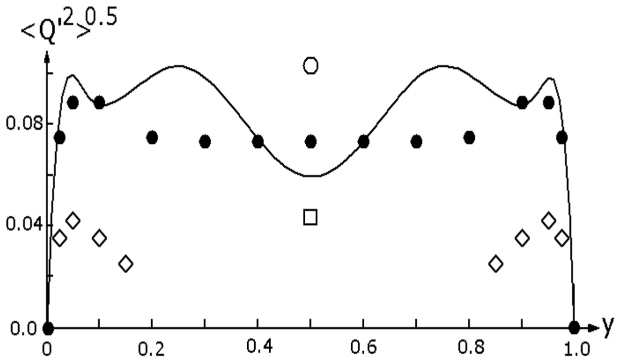

Figure 3
Rms of temperature pulsations at r = 1250

Figs.1-3, table 1 and [8] demonstrate that results of numerical 2-D simulation with free boundary conditions on the horizontal planes are consistent with experimental data in air and gaseous He.
Fig.4 represents the profile of rms temperature pulsations at r = 6000, here black solid line is result of present simulation (rigid), red and blue solid lines are theoretical laws [15].

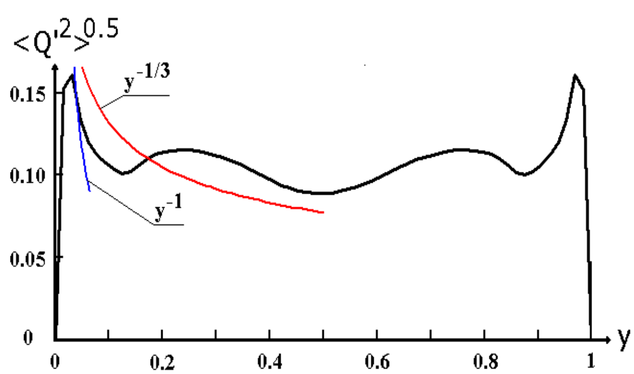

Figure 4
Rms of temperature pulsations at r = 6000

Fig.5 represents the profile of rms vertical velocity pulsations at r = 6000, here black solid line is result of present simulation (rigid), symbols ● and ● - experimental result [16] at r = 7300 and r = 18900, respectively (water, Pr = 6.1, aspect ratio is equal to 4.5 and $Ra_{cr} \approx 1820$ [17], result is recalculated using $v' \sim r^{0.44} \cdot Pr^{0.333}$ for scale [16]), magenta line is theoretical law [15].

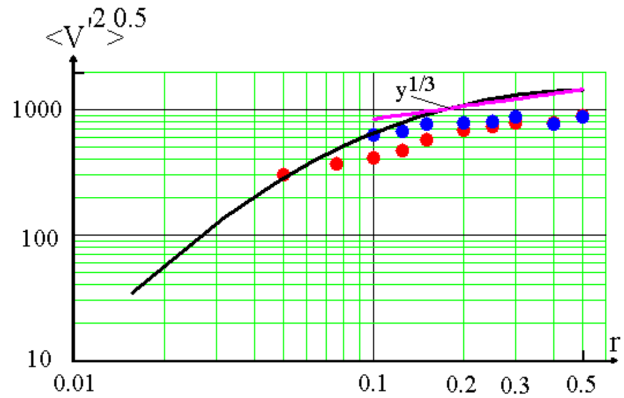

Figure 5
Rms of vertical velocity pulsations at r = 6000

Fig.6 represents the values of rms vertical velocity pulsations in centre between the planes divided by $Pr^{1/3}$, here green solid line – experimental result of [16] (water, Pr = 6.1), symbol ● - present numerical simulations (rigid, Pr = 10), symbol ● – experimental result of [7] (air, Pr = 0.71) and symbol ● – experimental result of [18] (water, Pr = 6.1).

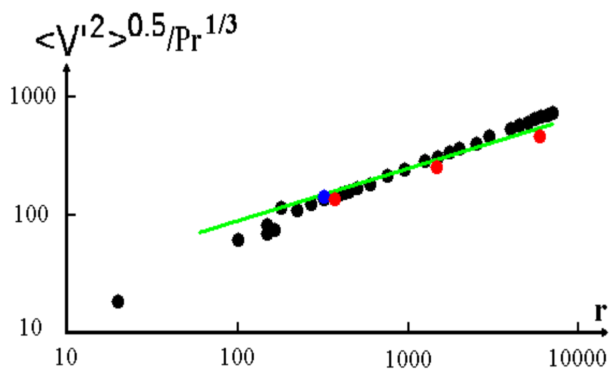

Figure 6
Rms of vertical velocity pulsations in centre

Table 2
Comparing of Nusselt Number at r = 4000

Work	Nu	Deviation in %
Present, rigid	16.9	0
O'Toole&Silveston, 1961 [20]	15.3	-9.5

In table 2 we compare the calculating Nusselt number and experimental data on turbulent convection in water. The agreement is good, but our numerical result is slightly higher.

Figs.4-6 and table 2 demonstrate that results of numerical 2-D simulation with rigid boundary conditions on the horizontal planes are consistent with experimental data in water and theoretical laws.

For free boundary conditions on horizontal plates, the values of Nusselt number at r > 700 describe by formula:

$$Nu = 1.223 \cdot r^{0.302},$$

This law practically coincides with experimental laws from [19] ($Nu = 1.222 \cdot r^{0.3}$) and O'Toole and Silveston, 1961 [20] ($Nu = 1.222 \cdot r^{0.305}$) and close to experimental law [12] ($Nu = 1.211 \cdot r^{0.3}$). The same power law has been derived also in numerical simulation [3] ($Nu \sim r^{0.301}$, infinite Prandtl number model, 2-D, free).

For rigid boundary conditions on horizontal plates, the values of Nusselt number at r > 300 describe by formula:

$$Nu = 1.323 \cdot r^{0.306}.$$

In recent experimental work [21] was found that $Nu \sim Ra^{0.309}$, in some experimental and numerical works the other laws were found – close to $Nu \sim r^{2/7}$ [5,11,13,14,16] and close to $Nu \sim r^{1/3}$ [22]. The detail review of experimental Nu-Ra laws may be found in work [22] (see also [20]).

TIME AND SPACE SPECTRUMS

Fig.7 represents the time spectrum of temperature pulsations in center of cell, here solid line is result of present simulation (free, r = 6500), blue points are experimental data [23] (gaseous He, $Ra = 1.1 \cdot 10^8$, $r \approx 6400$, $Ra_{cr} \approx 17000$ at aspect ratio is equal to 0.5 [17]). Normalizations are same. Frequency f is in unit of ν/H^2.

The green line represents the experimentally defined boundary of two regimes:

$$f_o = 0.05 \cdot Ra^{0.5} / \Pr,$$

above the frequency f_0 a power law has slope –1.4 (Obukhov-Bolgiano spectrum), and below f_0 the spectrum is flat.

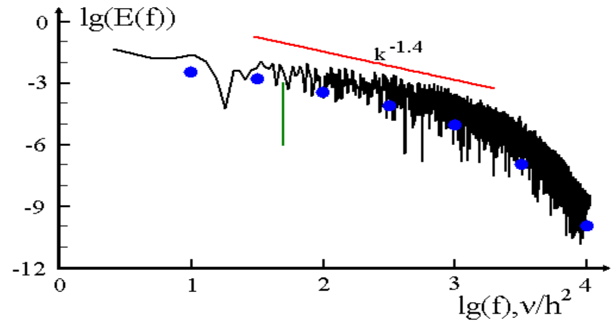

Figure 7
Time spectrum of temperature pulsations (free)

Figs.8 and 9 represent the one-dimensional space spectrums of temperature pulsations:

$$E_1(k) = \frac{1}{T}\int_0^T \{\sum_m \mathrm{Q(t)}^2{}_{\mathrm{km}}\}dt,$$

$$E_2(m) = \frac{1}{T}\int_0^T \{\sum_k \mathrm{Q(t)}^2{}_{\mathrm{km}}\}dt,$$

$$\mathrm{Q(t,x,y)} = \sum \mathrm{Q(t)}_{\mathrm{km}} \sin(\alpha kx)\sin(\pi my).$$

Here black points are result of present simulation (free, r = 26000).

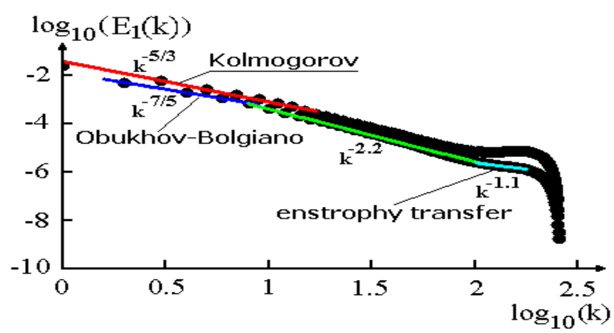

Figure 8
$E_1(k)$ space spectrum of temperature (free)

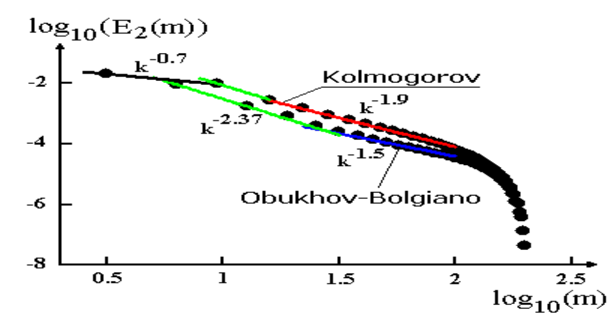

Figure 9
$E_2(m)$ space spectrum of temperature (free)

We can see the Kolmogorov ($k^{-5/3}$), Obukhov-Bolgiano ($k^{-7/5}$) and $k^{-2.4}$ spectrums earlier observed in experimental investigations of turbulent convection of gaseous He [21,23]. Fig.9 shows the slightly distorted spectrums of Kolmogorov and Obukhov-Bolgiano. Part k^{-1} is range of enstrophy transfer inherent to 2-D turbulent flows. It is surprising that ranges of $k^{-5/3}$ and $k^{-7/5}$ spectrums are partially coincident.

Fig.10 represents the one-dimensional space spectrum of temperature pulsations $E_2(m)$ for problem with rigid boundary conditions, here points are result of present simulation (r = 6000).

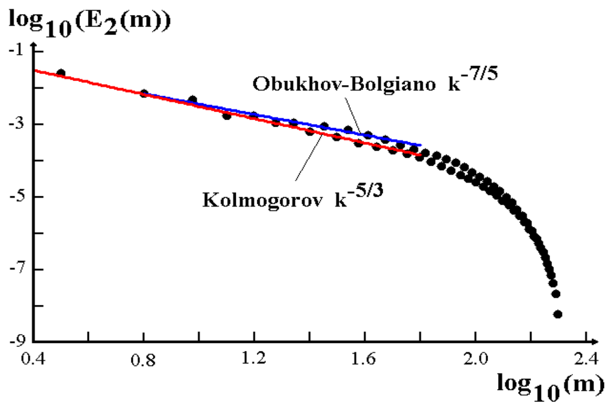

Figure 10

$E_2(m)$ space spectrum of temperature (rigid)

We can see also the Kolmogorov ($k^{-5/3}$), Obukhov-Bolgiano ($k^{-7/5}$) spectrums.

We calculated also the one-dimensional spectrum of kinetic energy $EK_2(m)$ by analogous formula. Fig. 11 shows the one-dimensional spectrums of kinetic energy $EK_2(m)$ for rigid (r = 6000) boundary conditions.

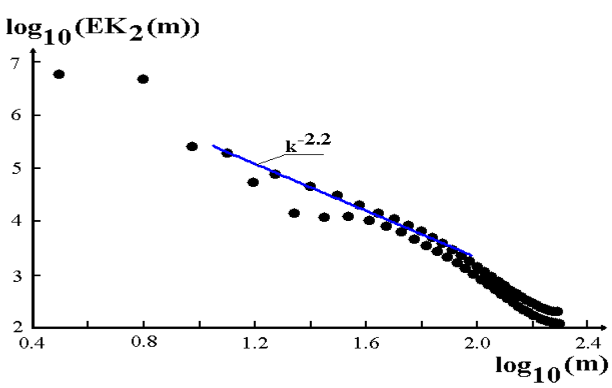

Figure 11

$EK_2(m)$ space spectrum of kinetic energy (rigid)

We can see the Obukhov-Bolgiano spectrum $k^{-2.2}$ for kinetic energy.

CONCLUSION

We compare the results of our 2-D simulations with free and rigid boundary conditions on the horizontal planes and experimental data on turbulent convection. Prandtl number is equal to 10 in a both simulations.

It is revealed that results of simulations with free boundary conditions have a good agreement with experimental data on turbulent convection in air and gaseous He. The profiles of mean temperature, rms of temperature and vertical velocity pulsations are close at enough high supercriticality. We observe also a good agreement with experimental data in time spectrum of temperature pulsations in centre of cell. The Nusselt numbers are close too.

The results of simulations with rigid boundary conditions have a reasonable agreement with experimental data on turbulent convection in water. The profiles of rms of temperature and vertical velocity pulsations are close to experimental data and theoretical laws. The Nusselt numbers at rigid boundary conditions are slightly higher, but exponent of the Nu-Ra power law is same for free and rigid simulations.

We studied the time and space spectrums of temperature pulsations and kinetic energy in both free and rigid simulations. The Kolmogorov ($k^{-5/3}$), Obukhov-Bolgiano ($k^{-7/5}$ for temperature pulsations and $k^{-11/5}$ for kinetic energy of pulsations) and $k^{-2.4}$ spectrums have been derived in our simulations. These spectrums were observed earlier in experimental investigations of turbulent convection of gaseous He. It is surprising that ranges of $k^{-5/3}$ and $k^{-7/5}$ spectrums are partially coincident.

REFERENCES (ЛИТЕРАТУРА)

1. Palymskiy, I. B., 2003, Determinism and Chaos in the Rayleigh-Benard Convection, Proceeding of the Second International Conference on Applied Mechanics and Materials (ICAMM 2003), Durban, South Africa, pp.139-144; http://palymsky.narod.ru/

2. Cortese T. and Balachandar S., 1993, Vortical Nature of Thermal Plumes in Turbulent Convection, Phys. Fluids, A 5(12), pp.3226-3232.

3. Malevsky A.V. and Yuen D.A., 1991, Characteristics-based Method Applied to Infinite Prandtl Number Thermal Convection in the Hard Turbulent Regime, Phys. Fluids A 3 (9), pp.2105-2115.
4. Werne, J., DeLuca, E.E. and Rosner, R., 1990, Numerical Simulation of Soft and Hard Turbulence: Preliminary Results for Two-Dimensional Convection, Phys. Rev. Lett., 64(20), pp.2370-2373.
5. Kerr, R.M., 1996, Rayleigh Number Scaling in Numerical Convection, J. Fluid Mech., 310, pp.139-179.
6. Grotzbach, G., 1982, Direct Numerical Simulation of Laminar and Turbulent Benard Convection, J. Fluid Mech., 119, pp.27-53 and Woerner, M., 1997 on web site:
http://hikwww4.fzk.de/irs/anlagensicherheit_und_systemsimulation/fluid_dynamics/simulation/e_index.html
7. Deardorff, J.W. and Willis, G.E., 1967, Investigation of Turbulent Thermal Convection Between Horizontal Plates, J. Fluid Mech., 28, pp. 675-704.
8. Palymskiy, I. B., Direct Numerical Simulation of Turbulent Convection, in book: Progress in Computational Heat and Mass Transfer, R. Bennacer (editor), vol.1, pg. 101-106, Lavoisier, 2005, http://palymsky.narod.ru/Paris.htm
9. Palymskiy, I.B., 2000, Metod Chislennogo Modelirovaniya Konvektivnykh Techeniy, Vychislitel'nye texnologii, 5, pp.53-61;
http://palymsky.narod.ru/
10. Palymskiy, I.B., 2004, Linejnyj I Nelinejnyj Analiz Chislennogo Metoda Rasscheta Konvektivnykh Techenij, Sibirskij Zhurnal Vychislitel'noj Matematiki, 7(2), pp. 143-163;
http://palymsky.narod.ru/
11. Threlfall, D. C., 1975, Free Convection in Low-Temperature Gaseous Helium, J. Fluid Mech., 67(1), pp.17-28.
12. Fitzjarrald, D.E., 1976, An Experimental Study of Turbulent Convection in Air, J. Fluid Mech., 73, pp.693-719.
13. Chu, T.Y. and Goldstein, R.J., 1973, Turbulent Convection in a Horizontal Layer of Water, J. Fluid Mech., 60(1), pp.141-159.
14. Wu, X.-Z. and Libchaber, A., 1992, Scaling Relations in Thermal Turbulence: The Aspect-Ratio Dependence, Physical Review, A 45(2), pp.842-845.
15. Kraichnan, R.H., 1962, Turbulent Thermal Convection at Arbitrary Prandtl Number, Phys. Fluids, 5 (11), pp. 1374-1389.
16. Garon, A.M. and Goldstein, R.J., 1973, Velocity and heat transfer measurements in thermal convection, Phys. Fluids, 16(11), pp. 1818-1825.
17. Gershuni, G.Z. and Zhuchovitskii, E.M.,1972, Konvektivnaya ustojchivost' neszhimaemoj zhidkosti, Nauka, Moskva, 1972.
English translation of this book:
Gershuni, G.Z. and Zhukhovitskii, E.M., 1976, Convective Stability of Incompressible Fluids, Israel Program for Scientific Translations, Jerusalem, 1976.
18. Malkus, W.V.R., 1954, Discrete Transitions in Turbulent Convection, Proc. Roy. Soc., A 225, pp.185-195.
19. Rossby, H. T., 1969, A Study of Benard Convection With and Without Rotation, J. Fluid Mech., 36, pp.309-335.
20. Denton, R.A. and Wood, I.R., 1979, Turbulent Convection Between Two Horizontal Plates, Int. J. Heat and Mass Transfer, 22, pp. 1339-1346.
21. Niemela, J. J., Skrbek, L., Sreenivasan, K. R. and Donnelly, R. J., 2000, Turbulent Convection at Very High Rayleigh Numbers, Nature, 404(20), pp. 837-840.
22. Fleischer, A. S. and Goldstein, R. S., 2002, High-Rayleigh-Number Convection of Pressurized Gases in a Horizontal Enclosure, J. Fluid Mechanics, 469, pp. 1-12.
23. Wu, X.-Z., Kananoff, L., Libchaber, A. and Sano, M., 1990, Frequency power Spectrum of Temperature Fluctuations in Free Convection, Physical Review Letters, 64(18), pp.2140-2143.

Igor Palymskiy *is Professor of Modern University for Humanities, Novosibirsk Branch, Mathematics Department. His main scientific interests are Direct Numerical Simulation of Turbulent Flows and Flows with Hydrodynamical Instabilities.*